On model for three-dimensional flow of nanofluid: An application to solar energy

Junaid Ahmad Khan [a], M. Mustafa [d], T. Hayat [b,c,*], M. Asif Farooq [d], A. Alsaedi [c], S.J. Liao [e]

[a] Research Centre for Modeling and Simulation (RCMS), National University of Sciences and Technology (NUST), Islamabad 44000, Pakistan
[b] Department of Mathematics, Quaid-I-Azam University, 45320, Islamabad 44000, Pakistan
[c] Department of Mathematics, Faculty of Science, King Abdulaziz University, P. O. Box 80257, Jeddah 21589, Saudi Arabia
[d] School of Natural Sciences, National University of Sciences and Technology (NUST), Islamabad 44000, Pakistan
[e] Department of Mathematics & State Key Lab of Ocean Engineering, School of Naval Architecture, Ocean and Civil Engineering, Shanghai Jiao Tong University, China

ARTICLE INFO

ABSTRACT

Laminar three-dimensional flow of nanofluid over a bi-directional stretching sheet is investigated. Convective boundary conditions are used for the analysis of thermal boundary layer. Mathematical model containing the combined effects of Brownian motion and thermophoretic diffusion of nanoparticles is adopted. The formulated differential system is solved numerically using a shooting method with fourth–fifth-order Runge–Kutta integration technique. The solutions depend on various interesting parameters including velocity ratio parameter (λ), Brownian motion parameter (N_b), thermophoresis parameter (N_t), Prandtl number (Pr), Lewis number (Le) and the Biot number (γ). It is noticed that fields are largely influenced with the variations of these parameters. The results are compared with the existing studies for the two-dimensional flows and found in an excellent agreement. The study reveals that nanoparticles in the base fluid offer a potential in improving the convective heat transfer performance of various liquids.

1. Introduction

The nanofluids in view of the extraordinary thermal conductivity enhancement have been recognized useful in several industrial and engineering applications. One of the technological applications of nanoparticles that hold enormous promise is the use of heat transfer fluids containing suspensions of nanoparticles to confront cooling problems in the thermal systems. Solar power is a direct way of obtaining heat, water and electricity from the nature. Researchers concluded that heat transfer and solar collection processes can be improved through the addition of nanoparticles in the fluids. Use of nanofluids as coolants would allow for smaller size and better positioning of the radiators which eventually consumes less energy for overcoming resistance on the road. Nanoparticles in refrigerant/lubricant mixtures could enable a cost effective technology for improving the efficiency of chillers that cool large buildings. Also the classical heat transfer fluids such as ethylene glycol, water and engine oil have limited heat transfer capabilities due to their low thermal conductivity and thus cannot congregate with modern cooling requirements. On the other hand thermal conductivity of metals is extremely higher in comparison to the conventional heat transfer fluids. Masuda et al. [1] explored the variations in the thermal conductivities and viscosities of liquids through the dispersion of ultra-fine particles in the base fluids. Choi and Eastman [2] combined the conventional heat transfer fluids with nanometer sized metallic particles and observed a significant increase in the thermal conductivity of the resulting liquid which was termed as nanofluid. In another paper, Eastman et al. [3] discussed an abnormal increase in the thermal conductivity of ethylene glycol based nanofluids.

Buongiorno [4] studied the convective transport phenomena in nanofluids and concluded that out of the seven slip mechanisms only Brownian motion and thermophoretic diffusion of nanoparticles contribute to the massive increase in the absolute thermal conductivity of the liquids. He also developed a mathematical model for nanofluid flow which incorporates the simultaneous effects of Brownian motion and thermophoretic diffusion of nanoparticles. Kuznetsov and Nield [5] investigated the natural convective boundary-layer flow of a nanofluid past a vertical flat plate using Buongiorno's model. Cheng–Minkowycz problem for natural convection flow of nanofluid past a vertical plate embedded in a porous medium was studied by Nield and Kuznetsov [6]. The two-dimensional flow of nanofluid over a linearly stretching sheet was conducted by Khan and Pop [7]. They computed the numerical solutions of the developed differential system by Keller-box and provided a detailed analysis of Brownian motion and thermophoresis effects on the heat transfer characteristics. Makinde and Aziz [8] extended this work by considering convective boundary conditions. They showed that strength of convective heating has a significant impact on the thermal boundary layer. Rana and Bhargava [9] provided finite element solutions for two-dimensional flow of

* Corresponding author at: Department of Mathematics, Quaid-I-Azam University, 45320, Islamabad 44000, Pakistan. Tel.: +92 51 90642172.
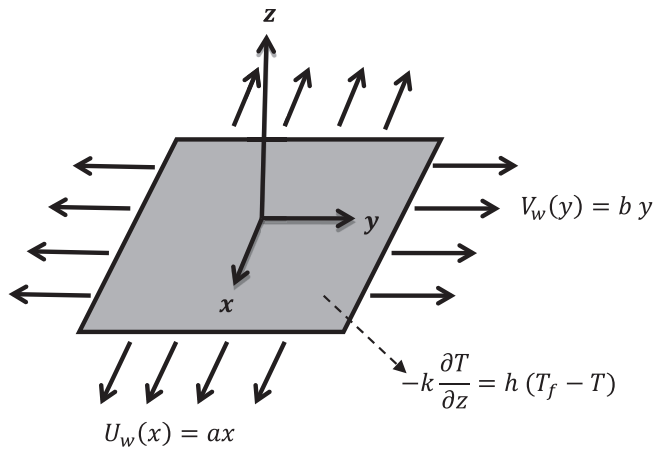E-mail address: pensy_t@yahoo.com (T. Hayat).

Fig. 1. Physical configuration and coordinate system.

nanofluid over a nonlinearly stretching sheet. Mustafa et al. [10] discussed stagnation-point flow of nanofluid towards a stretching surface by homotopy analysis method (HAM). In another paper Mustafa et al. [11] investigated the unsteady boundary layer flow of nanofluid past a stretching sheet. Flow of an electrically conducting nanofluid past a stretching cylinder was analyzed by Ashorynejad et al. [12]. Stagnation-point flow of nanofluid over a linearly stretching/shrinking surface was considered by Yacob et al. [13]. They have shown the existence of dual solutions in the case of shrinking sheet. Effect of internal heat generation on the nanofluid flow over a permeable stretching sheet was addressed by Hamad and Ferdows [14]. Free convective flow of nanofluid past a vertical flat surface with Newtonian heating boundary conditions was explored by Uddin et al. [15]. Khan and Pop [16] numerically investigated the forced convection flow of nanofluid through a porous medium using Brinkman–Forchheimer model. Numerical and analytic solutions for stagnation-point flow of nanofluid past an exponentially stretching sheet were provided by Mustafa et al. [17]. Stagnation-point flow of nanofluid past flat vertical plate with convective boundary conditions was examined by Makinde et al. [18]. MHD natural convection flow of nanofluid in a cavity is addressed by Sheikholeslami et al. [19]. Turkyilmazoglu and Pop [20] analyzed unsteady natural convection flow of nanofluid past a vertical infinite plate. MHD flow of nanofluid due to a rotating disk is studied by Rashidi et al. [21]. Nadeem and Haq [22] explored the MHD boundary layer flow over a permeable stretching sheet in the presence of nanoparticles.

Thermal radiation and viscous dissipation effects on the unsteady boundary layer flow of nanofluid over a stretching sheet were presented by Khan et al. [23]. Effect of solar energy radiation on the unsteady boundary layer flow of nanofluid past a wedge was discussed by Mohamad et al. [24]. They concluded that presence of nanoparticles in the base fluids allows deeper penetration of radiations. Sheikholeslami et al. [25] carried out an investigation to provide an application of LBM in simulation of natural convection nanofluid. The fluid fills the square cavity which has curve boundaries. Unsteady squeezing flow of nanofluid by ADM was investigated by Sheikholeslami et al. [26]. Turkyilmazoglu [27] provided both exact and analytical solutions for hydromagnetic flow of nanofluid with slip condition. In another investigation, Turkyilmazoglu [28] discussed the unsteady flow of nanofluid passing through a vertical plate.

The study of heat transfer in the boundary layer flows due to stationary or moving surface has relevance in various industrial applications. The seminal work on the laminar boundary flow over a flat plate at zero incidence in a quiescent ambient fluid with uniform free stream was reported by Blasius [29]. He provided an analytic solution of the problem in the power series form. The numerical solution to the Blasius problem was computed by Howarth [30]. In contrast to [29], the flow over a continuously moving plate was considered by Sakiadis [31]. Crane [32] extended this idea for a stretching sheet and provided an exact solution for the velocity distribution. The flow over a stretching sheet is involved in the extrusion process, fabrication of plastic, rubber and metallic sheets, glass and fiber production, wire drawing, hot rolling, melt spinning, transportation etc. In view of such applications, the Crane's problem has been extensively considered by the researchers even for the three-dimensional flows over a bi-directional stretching sheet. The seminal research in this direction was conducted by Wang [33]. He had also shown that classical problems of two-dimensional and axisymmetric flows due to stretching sheet can be easily recovered from his work. Unsteady three-dimensional flow past an impulsively stretching surface was analyzed by Lakshmisha et al. [34]. Series solutions for three-dimensional flow of an electrically conducting viscous fluid were provided by Xu et al. [35]. Sajid et al. [36] also derived analytic solutions for three-dimensional flow of elasto-viscous fluid over a stretching sheet. Liu and Andersson [37] numerically investigated the heat transfer characteristics over a bi-directional stretching sheet with variable wall temperature. Laminar three-dimensional flow of viscous fluid filling a porous space with heat and mass transfer was addressed by Hayat et al. [38]. The analytic solutions for three-dimensional flows of non-Newtonian fluids over a stretching sheet have been reported by Hayat et al. [39,40]. Recently Liu et al. [41] provided an interesting

Table 1
Comparison of values of reduced Nusselt number $-\theta'(0)$ with the previous studies when $N_b = N_t = 0$, $\lambda = 0$, $\gamma = 1000$.

Pr	Khan and Pop [7]	Makinde and Aziz [8]	Gorla and Sidawi [42]	Present (bvp4c)	Present (shooting method)
0.07	0.0663	0.0656	0.0656	0.06562	0.06562
0.20	0.1691	0.1691	0.1691	0.16909	0.16909
0.70	0.4539	0.4539	0.5349	0.45392	0.45392
2.00	0.9113	0.9114	0.9114	0.91136	0.91136
7.00	1.8954	1.8954	1.8905	1.89542	1.89542
20.00	3.3539	3.3539	3.3539	3.35394	3.35391
70.00	6.4621	6.4622	6.4622	6.46231	6.46220

Table 2
Comparison of values of the reduced Nusselt number $-\theta'(0)$ with Makinde and Aziz [8] with $Le = Pr = 10$, $\gamma = 0.1$, $\lambda = 0$.

| N_t	Nur ($N_b = 0.1$)	Nur ($N_b = 0.2$)	Nur ($N_b = 0.3$)	Nur ($N_b = 0.4$)	Nur ($N_b = 0.5$)
0.1	0.092907 (0.0929)	0.087332 (0.0873)	0.076878 (0.0769)	0.059665 (0.0597)	0.038325 (0.0383)
0.2	0.092732 (0.0927)	0.086762 (0.0868)	0.075082 (0.0751)	0.055349 (0.0553)	0.032498 (0.0325)
0.3	0.092545 (0.0925)	0.086119 (0.0861)	0.072917 (0.0729)	0.050269 (0.0503)	0.026905 (0.0269)
0.4	0.092344 (0.0923)	0.085385 (0.0854)	0.070265 (0.0703)	0.044558 (0.0445)	0.022010 (0.0220)
0.5	0.092126 (0.0921)	0.084538 (0.0845)	0.066974 (0.0700)	0.038620 (0.0386)	0.018035 (0.0180)
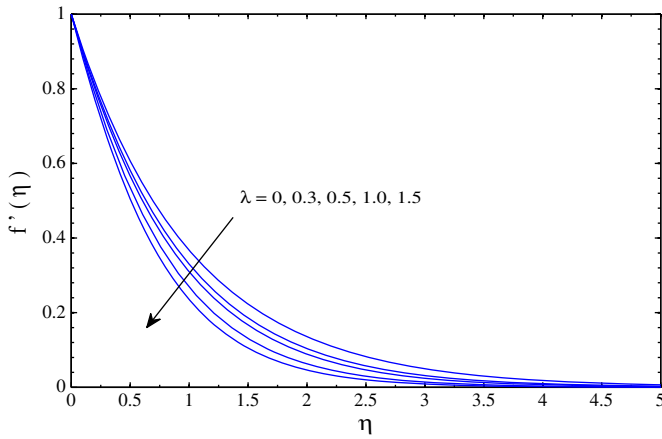
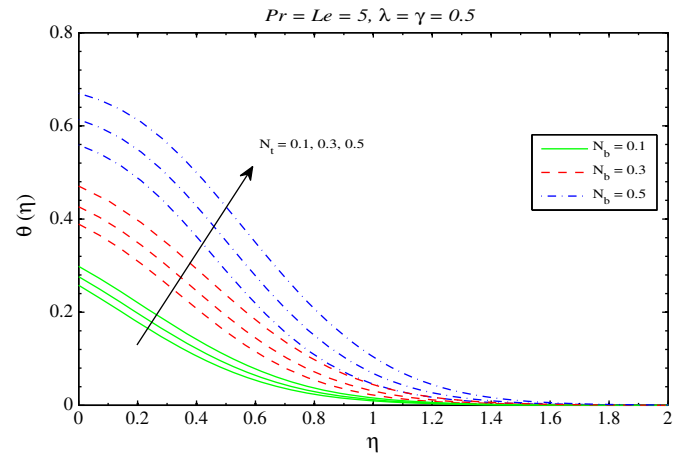**Fig. 2.** Effect of λ on f'.

Fig. 4. Effects of N_b and N_t on θ.

study on the three-dimensional flow and heat transfer over an exponentially stretching surface. In this work the wall temperature was also assumed to be of the exponential form.

To the best of our information, there is not a single article that considers the three-dimensional flow of nanofluid due a stationary or moving surface. The present work therefore describes the three-dimensional flow of nanofluid over a sheet which is stretched in two-lateral directions. Further the thermal boundary layer analysis is performed in the presence of convective boundary conditions. The developed nonlinear differential system has been solved numerically by shooting method with fourth–fifth order Runge–Kutta (RK45) integration technique. A comparative study of present results and the previously published ones in case of two-dimensional flow is presented. The results clearly indicate that nanoparticles in the base fluid can sufficiently improve the convective heat transfer performance.

2. Problem formulation

Let us consider the three-dimensional incompressible boundary layer flow of nanofluid over a convectively heated sheet located along the xy-plane and z-axis is chosen normal to the surface. The sheet is stretched in two lateral directions by keeping the origin fixed. The velocities of the sheet along x- and y-directions are respectively $U_w(x) = ax$ and $V_w(y) = by$ (see Fig. 1). Impacts of Brownian motion and thermophoretic diffusion of nanoparticles are considered in the transport equations. T_f denotes the convective surface temperature while T_∞ is the ambient fluid's temperature. The concentration of

nanoparticles at the sheet is denoted by C_w whereas C_∞ is the ambient concentration. Under the usual boundary layer assumptions, the equations governing the conservations of mass, momentum, energy and nanoparticles diffusion are

$$\frac{\partial u}{\partial x} + \frac{\partial v}{\partial y} + \frac{\partial w}{\partial z} = 0, \tag{1}$$

$$u\frac{\partial u}{\partial x} + v\frac{\partial u}{\partial y} + w\frac{\partial u}{\partial z} = \nu\frac{\partial^2 u}{\partial z^2}, \tag{2}$$

$$u\frac{\partial v}{\partial x} + v\frac{\partial v}{\partial y} + w\frac{\partial v}{\partial z} = \nu\frac{\partial^2 v}{\partial z^2}, \tag{3}$$

$$u\frac{\partial T}{\partial x} + v\frac{\partial T}{\partial y} + w\frac{\partial T}{\partial z} = \alpha\frac{\partial^2 T}{\partial z^2} + \tau\left[D_B\left(\frac{\partial C}{\partial z}\frac{\partial T}{\partial z}\right) + \frac{D_T}{T_\infty}\left(\frac{\partial T}{\partial z}\right)^2\right], \tag{4}$$

$$u\frac{\partial C}{\partial x} + v\frac{\partial C}{\partial y} + w\frac{\partial C}{\partial z} = \left[D_B\left(\frac{\partial^2 C}{\partial z^2}\right) + \frac{D_T}{T_\infty}\left(\frac{\partial^2 T}{\partial z^2}\right)\right], \tag{5}$$

where u, v and w are the velocity components along x, y and z-directions, ν is the kinematic viscosity, T is the fluid's temperature, C is the nanoparticle concentration, α is the thermal diffusivity, D_B is the Brownian diffusion coefficient, D_T is the thermophoretic diffusion coefficient and $\tau(= (\rho C)_p/(\rho C)_f)$ is the ratio of the effective heat capacity of the nanoparticle
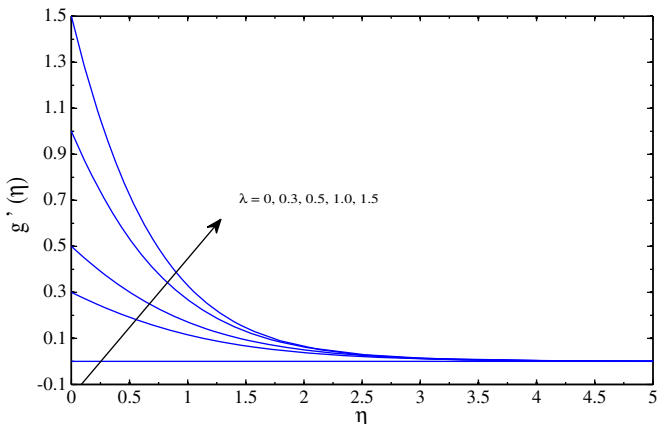

Fig. 3. Effect of λ on g'.
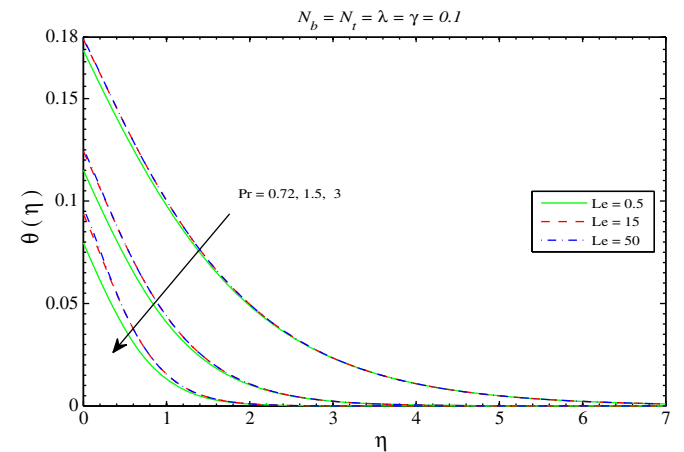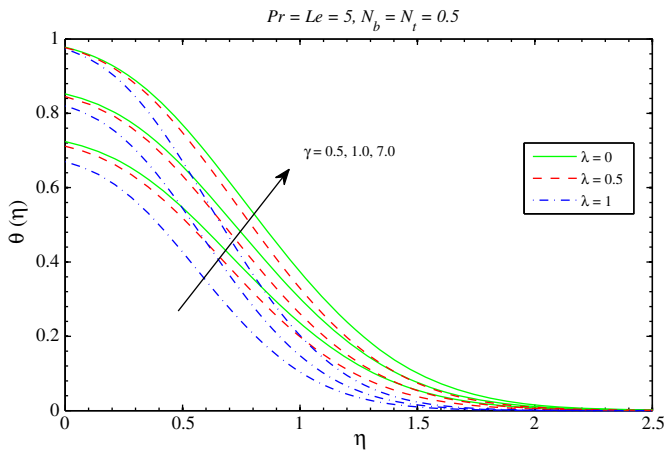

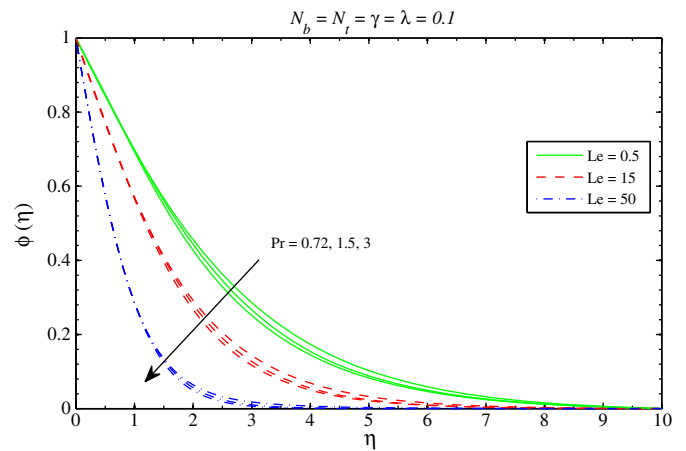**Fig. 5.** Effects of Pr and Le on θ.

Fig. 6. Effects of λ and γ on θ.

material to the effective heat capacity of the base fluid. The boundary conditions for the considered problem are

$$u = U_w(x) = ax, v = V_w(y) = by, w = 0, -k\frac{\partial T}{\partial z} = h(T_f - T), C = C_w \text{ at } z = 0, \tag{6}$$

$$u = 0, v = 0, T \to T_\infty, C \to C_\infty \text{ as } z \to \infty, \tag{7}$$

in which k is the thermal conductivity and h is the convective heat transfer coefficient. Using the following dimensionless variables

$$\eta = \sqrt{\frac{a}{\nu}}z, u = axf'(\eta), v = ayg'(\eta), w = -\sqrt{\nu a}(f+g), \tag{8}$$

$$\theta(\eta) = \frac{T-T_\infty}{T_f-T_\infty}, \phi(\eta) = \frac{C-C_\infty}{C_w-C_\infty}. \tag{9}$$

Eq. (1) is identically satisfied and Eqs. (2)–(7) become

$$f''' = -(f+g)f'' + f'^2, \tag{10}$$

$$g''' = -(f+g)g'' + g'^2, \tag{11}$$

$$\theta'' = -\text{Pr}(f+g)\theta' - \text{Pr}N_b\phi'\theta' - \text{Pr}N_t\theta'^2, \tag{12}$$

$$\phi'' = -Le(f+g)\phi' - \frac{N_t}{N_b}\theta'', \tag{13}$$

Fig. 8. Effects of Pr and Le on ϕ.

$$f(0) = g(0) = 0, f'(0) = 1, g'(0) = \lambda, \theta'(0) = -\gamma[1-\theta(0)], \phi(0) = 1, \tag{14}$$

$$f'(\infty) = g'(\infty) = 0, \theta(+\infty) \to 0, \phi(+\infty) \to 0, \tag{15}$$

where $\lambda = b/a$ is ratio of rates, $\gamma = \frac{h}{k}\sqrt{\frac{\nu}{a}}$ is the Biot number, $N_b = \tau D_B(C_w - C_\infty)/\nu$ is the Brownian motion parameter, $N_t = \tau D_T(T_w - T_\infty)/T_\infty\nu$ is the thermophoresis parameter, $Pr = \frac{\nu}{\alpha}$ is the Prandtl number and $Le = \frac{\nu}{D_B}$ is the Lewis number.

With the help of local Nusselt number $Nu_x = \frac{xq_w}{k(T_w-T_\infty)}$ and local Sherwood number $Sh = \frac{xj_w}{D_B(C_w-C_\infty)}$ one obtains

$$\frac{Nu_x}{\sqrt{Re_x}} = -\theta'(0) = Nur, \frac{Sh}{\sqrt{Re_x}} = -\phi'(0) = Shr, \tag{16}$$

where $Re_x = U_w(x)/\nu$ is the local Reynolds number and q_w and j_w are the wall heat and mass fluxes, respectively.

3. Numerical method

The dimensionless momentum, energy and concentration (Eqs. (10)–(13)) with the boundary conditions (Eqs. (14) and (15)) have been solved numerically by shooting method with fourth–fifth order Runge–Kutta (RK45) integration technique. First we reduce the original ODEs into a system of 1st order ODEs by setting $x_1 = f, x_2 = f'$,
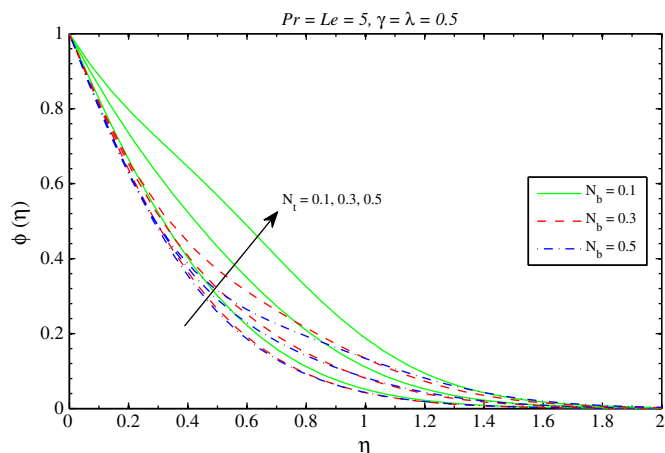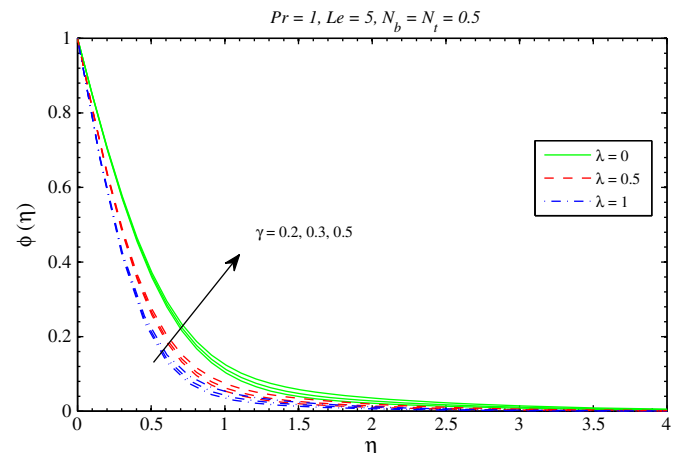

Fig. 7. Effects of N_b and N_t on ϕ.
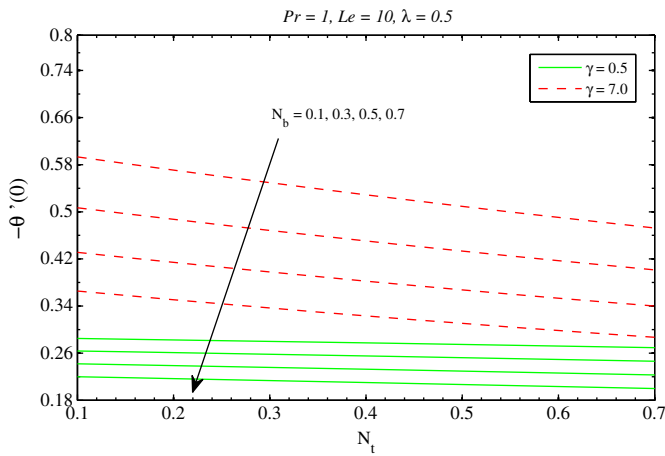

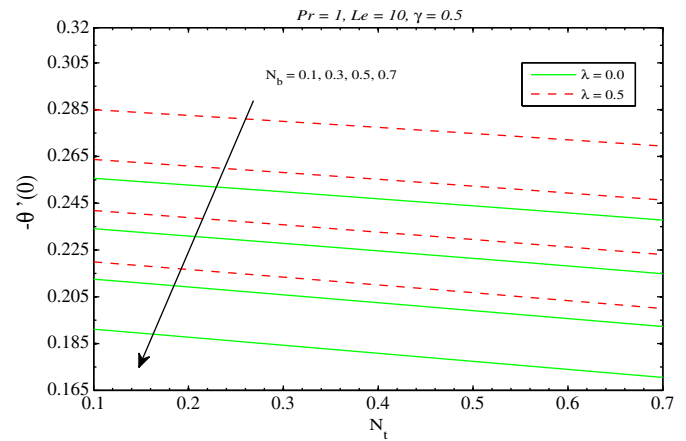**Fig. 9.** Effects of γ and λ on ϕ.

Fig. 10. Effects of N_b and N_t on *Nur* for different values of γ.

$x_3 = f''$, $x_4 = g$, $x_5 = g'$, $x_6 = g''$, $x_7 = \theta$, $x_8 = \theta'$, $x_9 = \phi$ and $x_{10} = \phi'$ which gives

$$
\begin{bmatrix} x_1' \\ x_2' \\ x_3' \\ x_4' \\ x_5' \\ x_6' \\ x_7' \\ x_8' \\ x_9' \\ x_{10}' \end{bmatrix} = \begin{bmatrix} x_2 \\ x_3 \\ -(x_1+x_4)x_3 + (x_2)^2 \\ x_5 \\ x_6 \\ -(x_1+x_4)x_6 + (x_5)^2 \\ x_8 \\ -\Pr\left((x_1+x_4)x_8 + N_b x_8 x_{10} + N_t(x_8)^2\right) \\ x_{10} \\ -Le(x_1+x_4)x_{10} - \dfrac{N_t}{N_b}x_8' \end{bmatrix}
\tag{17}
$$

and the corresponding initial conditions are

$$
\begin{bmatrix} x_1 \\ x_2 \\ x_3 \\ x_4 \\ x_5 \\ x_6 \\ x_7 \\ x_8 \\ x_9 \\ x_{10} \end{bmatrix} = \begin{bmatrix} 0 \\ 1 \\ u_1 \\ 0 \\ \lambda \\ u_2 \\ u_3 \\ -\gamma(1-u_3) \\ 1 \\ u_4 \end{bmatrix}.
\tag{18}
$$

Fig. 11. Effects of *Pr* and *Le* on *Nur* for different values of γ.

Fig. 12. Effects of N_b and N_t on *Nur* for different values of λ.

The set of Eq. (17) subject to the initial conditions (Eq. (18)) are solved using RK45 method. Suitable values of the unknown initial conditions u_1, u_2, u_3 and u_4 are approximated and optimized through Newton method until the boundary conditions at infinity (given in Eq. (15)) are satisfied. The computations have been done by using MATLAB. The maximum value of η_∞, to each group of parameters is determined when the values of unknown boundary conditions at $\eta = 0$ do not change to a successful loop with error less than 10^{-6}.

4. Results and discussion

To validate the solutions we have compared the values of $-\theta'(0)$ and $-\phi'(0)$ with those obtained by Khan and Pop [7], Makinde and Aziz [8] and Gorla and Sidawi [42] for the two-dimensional case ($\lambda = 0$) (see Tables 1 and 2). It is witnessed that solutions are in very good agreement for all the considered values of parameters. Figs. 2 and 3 show the velocity profiles for different values of ratio λ. It is quite obvious that increase in λ corresponds to either increase in the sheet velocity along y-direction or its decrease in the x-direction. Thus one would expect a decrease in the x-component of velocity and an increase in the y-component of velocity with an increase in λ. Fig. 4 shows the behaviors of Brownian motion and thermophoresis effects on the temperature distribution θ. Brownian motion takes place due to the size of nanoparticles which is of nanoscale and at this level the particle motion has a strong influence on the heat transfer. An increase in N_b leads to an increase in the nanoparticle motion and consequently the kinetic energy of these nanoparticles increase. The nanofluid's temperature is therefore an increasing function of N_b. Temperature θ also increases when N_t
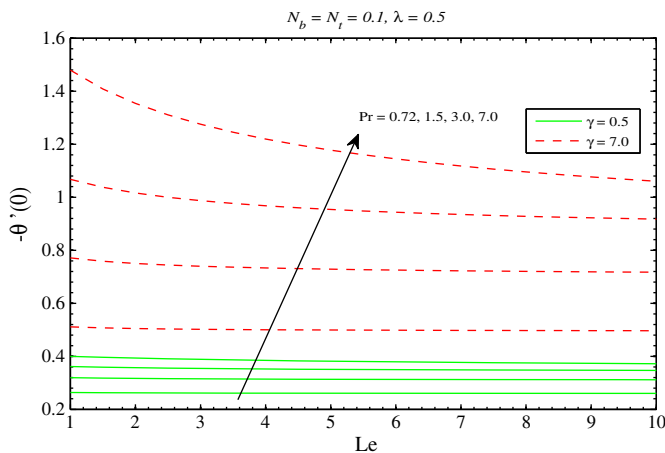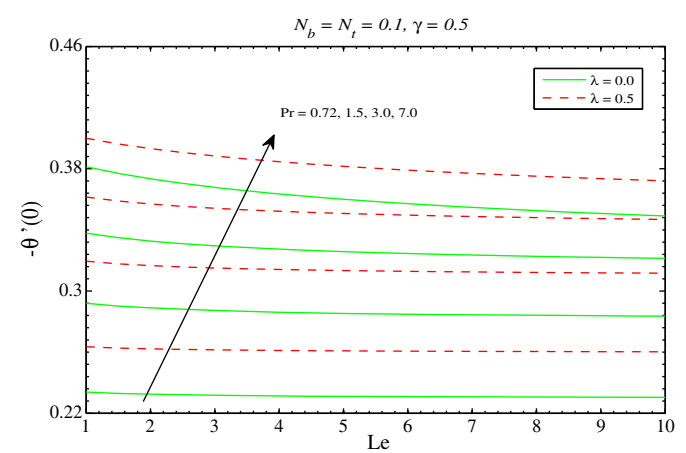

Fig. 13. Effects of *Pr* and *Le* on *Nur* for different values of λ.
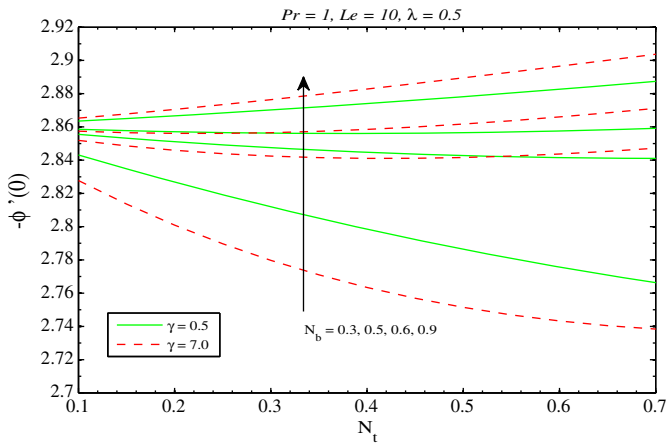
Fig. 14. Effects of N_b and N_t on Shr for different values of γ.
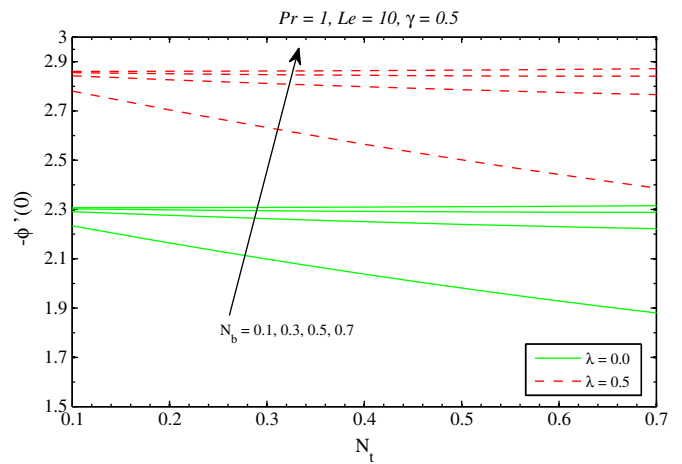

Fig. 16. Effects of N_b and N_t on Shr for different values of λ.

is increased for any chosen value of N_b. It is also seen that variation in the thermal boundary layer becomes pronounced as Brownian motion effect intensifies. Fig. 5 is prepared to see the variations in the temperature distribution with an increase in the Prandtl number Pr for different values of Lewis number Le. Prandtl number is defined as the ratio of momentum diffusivity to thermal diffusivity. Thus smaller values of $Pr(<1)$ correspond to the fluids which are highly conducive but have low viscosity such as air and other gases. On the other hand the fluids such as water, engine oils, and ethylene glycol have low thermal conductivity and therefore these are characterized by large values of $Pr(>1)$. As expected the thermal boundary layer thins and the temperature profiles become steeper when Pr is increased. Thus decrease in the thermal boundary layer with an increase in Pr accompanies with the larger rate of heat transfer at the sheet. It is also found that variation in the Lewis number Le only affects the temperature distribution closer to the stretching sheet (which is in accordance with Makinde and Aziz [8]). The impact of convective heating on the thermal boundary layer is seen in Fig. 6. It is evident that increase in the Biot number γ corresponds to a stronger convective heating at the sheet which allows a deeper penetration of thermal effect in the quiescent fluid. As a consequence the temperature increases and thermal boundary layer becomes thicker with an increase in γ. The results for constant wall temperature case ($\theta(0) = 1$) (obtained by assuming sufficiently large values of γ) are also given. Variations in the temperature profiles are almost similar for all the considered values of λ. However temperature θ decreases with an increase in λ.

The combined influence of Brownian motion and thermophoresis effects on the concentration ϕ is depicted in Fig. 7. An increase in N_t

corresponds to an increase in the nanoparticle concentration and a decrease in the wall slope of the concentration ϕ. This outcome is only true for smaller Lewis number for which the Brownian diffusion effect is large compared to convection. However for large Lewis number ($Le = 1000$), an increase in the thermophoretic effect would limit the penetration depth for concentration boundary layer. For smaller Brownian motion the profiles become steeper when N_t is increased whereas opposite trend is accounted for a stronger Brownian motion. Fig. 8 illustrates that increase in Le accompanies with the weaker Brownian diffusion coefficient D_B and shorter penetration depth for concentration boundary layer. The pattern for nanoparticle volume fraction is almost similar for all the considered values of Pr. Influence of Biot number γ on the concentration ϕ is anticipated in Fig. 9. It is already witnessed from Fig. 6 that temperature θ rises when the convective heating at the sheet is enhanced. The concentration field ϕ, being driven by the temperature field, therefore increases with an increase in γ.

Figs. 10–13 are sketched to perceive the effects of different parameters on the reduced Nusselt number Nur. We earlier noticed in Fig. 4 that profiles become flat near the stretching wall when N_b changes from 0.1 to 0.3 revealing a decrement in the initial slopes. The variation in the wall temperature gradient $|\theta'(0)|$ with N_b and N_t becomes prominent as the convective surface heating is increased (see Fig. 10). It is observed that wall temperature gradient $|\theta'(0)|$ decreases with an increase in N_t for a weaker Brownian motion. This decrease becomes much significant when N_b changes from 0.1 to 0.5. This is because strengthened
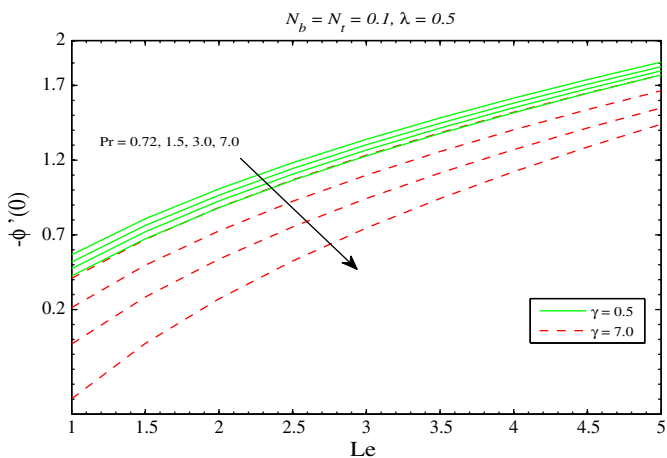

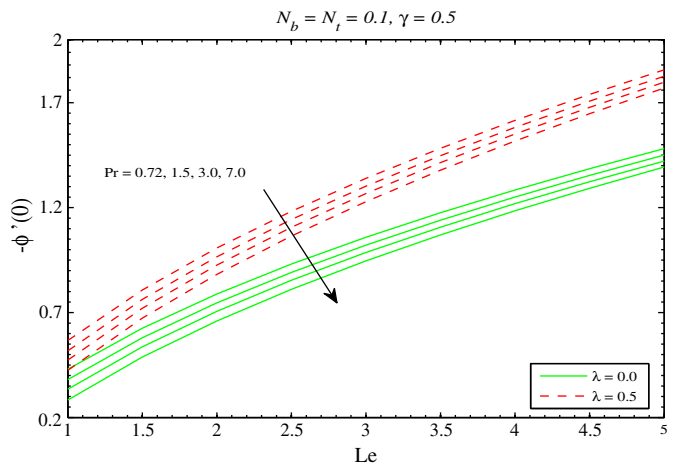**Fig. 15.** Effects of Pr and Le on Shr for different values of γ.

Fig. 17. Effects of Pr and Le on Shr for different values of λ.

Brownian motion corresponds to the intense motion of nanoparticles which are driven from the stretching wall to the quiescent fluid. It can also be seen that reduced Sherwood number Shr is inversely proportional to the thermophoresis parameter N_t. This is due to the fact that hot stretching sheet repels the ultra-fine particles from it, thereby forming a particle-free layer near the surface. Fig. 11 plots the wall temperature gradient versus Le for different values of Pr. The variations in $|\theta'(0)|$ with Le are only significant in case of a smaller Prandtl number fluid. A decrease in the thermal boundary layer thickness with an increase in Pr meets with the larger heat transfer rate near the sheet. It is also indicated that variations in Nur with N_b, N_t, Pr and Le are similar for two-dimensional, three-dimensional and axisymmetric flows. Figs. 14–17 show the plots for wall concentration gradient $|\phi'(0)|$ for the data given in Figs. 10–13. It is revealed that wall mass flux is significantly influenced by the variation of parameters in case of strong convective heating. Moreover the obtained results are in accordance with Makinde and Aziz [8] for the two-dimensional flow.

5. Conclusions

Three-dimensional flow with nanoparticles over a bi-directional stretching sheet is studied in the presence of convective boundary conditions. The resulting differential system is solved for the numerical solutions by Runge–Kutta method using a shooting technique. The key points of this work are as under:

a. The x-component of velocity f' is an increasing function of λ. However y-component of velocity g' increases when λ is increased.
b. Increasing values of Pr corresponds to a decrease in the thermal diffusivity and thinner boundary layer. The thermal boundary layer decreases. The decrease in the thermal boundary layer is compensated with an increase in the rate of heat transfer at the stretching sheet. The Lewis number Le has a negligible impact on the thermal boundary layer.
c. Intensification in the Brownian motion and thermophoresis effects enhances the temperature and thermal boundary layer thickness. Whereas the nanoparticle volume fraction is found to decrease upon increasing the Brownian motion parameter.
d. The dimensionless wall temperature and concentration gradients are greater in the three-dimensional flow when compared with the two-dimensional flow case.
e. The obtained solutions are in excellent agreement with Khan and Pop [7], Gorla and Sidawi [42] and Makinde and Aziz [8] for two-dimensional flow ($\lambda = 0$) with constant wall temperature case ($\theta(0) = 1$).

Acknowledgment

References

[1] H. Masuda, A. Ebata, K. Teramae, N. Hishinuma, NetsuBussei (in Japanese) 4 (1993) 227–233.
[2] S.U.S. Choi, J.A. Eastman, The Proceedings of the 1995 ASME International Mechanical Engineering Congress and Exposition, San Francisco, USA, ASME, FED 231/MD, 66, 1995, pp. 99–105.
[3] J.A. Eastman, S.U.S. Choi, S. Li, W. Yu, L.J. Thompson, Appl. Phys. Lett. 78 (2001) 718–720.
[4] J. Buongiorno, ASME J. Heat Transfer 128 (2006) 240–250.
[5] A.V. Kuznetsov, D.A. Nield, Int. J. Therm. Sci. 49 (2010) 243–247.
[6] D.A. Nield, A.V. Kuznetsov, Int. J. Heat Mass Transf. 52 (2009) 5792–5795.
[7] W.A. Khan, I. Pop, Int. J. Heat Mass Transf. 53 (2010) 2477–2483.
[8] O.D. Makinde, A. Aziz, Int. J. Therm. Sci. 50 (2011) 1326–1332.
[9] P. Rana, R. Bhargava, Commun. Nonlinear Sci. Numer. Simul. 17 (2012) 212–226.
[10] M. Mustafa, T. Hayat, I. Pop, S. Asghar, S. Obadiat, Int. J. Heat Mass Transfer 54 (2011) 5588–5594.
[11] M. Mustafa, T. Hayat, A. Alsaedi, J. Mech. 29 (2013) 423–432.
[12] H.R. Ashorynejad, M. Sheikholeslami, I. Pop, D.D. Ganji, Heat Mass Transfer 49 (2013) 427–436.
[13] N.A. Yacob, A. Ishak, I. Pop, K. Vajravelu, Boundary layer flow past a stretching/shrinking surface beneath an external uniform shear flow with a convective surface boundary condition in a nanofluid, Nanoscale Res. Lett. 6 (2011) 314.
[14] M.A.A. Hamad, M. Ferdows, Commun. Nonlinear Sci. Numer. Simul. 17 (2012) 132–140.
[15] M.J. Uddin, W.A. Khan, A.I. Ismail, PLoS One 7 (2012), http://dx.doi.org/10.1371/journal.pone.0049499.
[16] W.A. Khan, I. Pop, PLoS One 7 (2012), http://dx.doi.org/10.1371/journal.pone.0047031.
[17] M. Mustafa, M.A. Farooq, T. Hayat, A. Alsaedi, PLoS One 8 (2013), http://dx.doi.org/10.1371/journal.pone.0061859.
[18] O.D. Makinde, W.A. Khan, Z.H. Khan, Int. J. Heat Mass Transf. 62 (2013) 526–533.
[19] M. Sheikholeslami, M. Gori-Bandpy, D.D. Ganji, S. Soleimani, J. Taiwan Inst. Chem. Eng. (2014), http://dx.doi.org/10.1016/j.jtice.2013.06.019.
[20] M. Turkyilmazoglu, I. Pop, Int. J. Heat Mass Transfer 59 (2013) 167–171.
[21] M.M. Rashidi, S. Abelman, N.F. Mehr, Int. J. Heat Mass Transfer 62 (2013) 515–525.
[22] S. Nadeem, R.U. Haq, J. Aerosp. Eng. (2012), http://dx.doi.org/10.1061/(ASCE)AS.1943-5525.0000299.
[23] M.S. Khan, I. Karim, L.E. Ali, I. Islam, Int. Nano Lett. 24 (2012) 1–9.
[24] R.B. Mohamad, R. Kandasamy, I. Muhaimin, Heat Mass Transf. 49 (2013) 1261–1269.
[25] M. Sheikholeslami, M. Gorji-Bandpy, S.M. Seyyedi, D.D. Ganji, H.B. Rokni, S. Soleimani, Powder Technol. 247 (2013) 87–94.
[26] M. Sheikholeslami, D.D. Ganji, H.R. Ashorynejad, Powder Technol. 239 (2013) 259–265.
[27] M. Turkyilmazoglu, Chem. Eng. Sci. 84 (2012) 182–187.
[28] M. Turkyilmazoglu, J. Heat Transfer-Trans. ASME (2014), http://dx.doi.org/10.1115/1.4025730 (in press).
[29] H. Blasius, Z. Math. Phys. 56 (1908) 1–37.
[30] L. Howarth, Proc. R. Soc. Lond. A 164 (1938) 547–579.
[31] B.C. Sakiadis, AIChE J 7 (1961) 26–28.
[32] L.J. Crane, J. Appl. Math. Phys. (ZAMP) 21 (1970) 645–647.
[33] C.Y. Wang, Phys. Fluids 27 (1984) 1915–1917.
[34] K.N. Lakshmisha, S. Venkateswaran, G. Nath, ASME-J. Heat Transfer 110 (1988) 590.
[35] H. Xu, S.J. Liao, I. Pop, Eur. J. Mech. B. Fluids 26 (2007) 15–27.
[36] M. Sajid, T. Hayat, I. Pop, Nonlinear Anal. Real World Appl. 9 (2008) 1811–1822.
[37] I.C. Liu, H.I. Andersson, Int. J. Heat Mass Transfer 51 (2008) 4018–4024.
[38] T. Hayat, M. Qasim, Z. Abbas, Commun. Nonlinear Sci. Numer. Simul. 15 (2010) 2375–2387.
[39] T. Hayat, M. Mustafa, M. Sajid, Numer. Meth. Partial Differ. Equ. 27 (2011) 915–936.
[40] T. Hayat, M. Awais, A. Safdar, A.A. Hendi, Nonlinear Anal. Model. Cont. 17 (2012) 47–59.
[41] I.C. Liu, H.H. Wang, Y.F. Peng, Chem. Eng. Commun. 200 (2013) 253–268.
[42] R.S.R. Gorla, I. Sidawi, Appl. Sci. Res. 52 (1994) 247–257.